JACS
JOURNAL OF THE AMERICAN CHEMICAL SOCIETY
Article
pubs.acs.org/JACS

Phase-Controlled Synthesis of Cu_2ZnSnS_4 Nanocrystals: The Role of Reactivity between Zn and S

Yu Zou,[†] Xiong Su,[‡] and Jiang Jiang*,[†]

[†]i-Lab and Division of Nanobiomedicine, Suzhou Institute of Nano-Tech and Nano-Bionics, Chinese Academy of Sciences, Suzhou, People's Republic of China 215123

[‡]Department of Biochemistry and Molecular Biology, Medical College of Soochow University, Suzhou, People's Republic of China 215123

Supporting Information

ABSTRACT: Cu_2ZnSnS_4 (CZTS) nanocrystals with different morphologies and phases have been synthesized in hot organic solvents such as dodecanethiol and oleylamine. The crystallographic phases could be controlled by the sulfur precursor and the ligand species of the metal salts used for the synthesis. When a highly reactive sulfur precursor and metal acetates were used, wurtzite CZTS nanocrystals were obtained. On the other hand, using a low-reactivity sulfur precursor or metal chlorides produced CZTS nanocrystals in a kesterite phase. The experimental results from systematic investigations indicated that the reaction rate between Zn and S precursors played a determining role for the growth of CZTS nanocrystals with different crystalline phases. A relatively faster reaction between Zn and S precursors in comparison to the Sn−S reaction favored the formation of a metastable wurtzite phase, which could be accelerated by increasing the reactivity of the S precursor. This work provided a safe and economical way to synthesize high-quality phase-controlled Cu_2ZnSnS_4 nanocrystals, especially wurtzite nanorods, for potential photovoltaic applications. Moreover, preliminary results show that the proposed mechanism also applies to the phase-controlled synthesis of other quaternary Cu_2MSnS_4 (M = Cd^{2+}, Mn^{2+}) nanocrystals.

INTRODUCTION

Photovoltaic devices based on colloidal semiconductor nanocrystals have been intensely studied in the past decade due to their low cost and potentially high efficiency.[1,2] Cadmium chalcogenides, lead chalcogenides, and ternary copper-based chalcopyrite nanocrystals are the most studied nanocrystal light absorbers to date. However, the practical use of these nanocrystals for photovoltaic applications may be restricted because they contain either toxic or relatively rare elements.[3] To overcome these limitations, quaternary Cu_2ZnSnS_4 (CZTS) nanocrystals consisting of only earth-abundant elements with low toxicity have attracted considerable attention.[4−6] As a direct band gap semiconductor with an optimal band gap of ∼1.5 eV and a large absorption coefficient of $\sim 10^4$ cm^{-1}, CZTS is expected to be an ideal solar cell absorber.[7,8] A recent report has demonstrated that photoelectric conversion efficiency of solar cells fabricated using CZTS nanocrystals reached 7.2%,[9] showing the great promise of this material in photovoltaic applications. The nanoparticle crystalline phase and morphology may influence the band gaps and device fabrications, which in turn will affect the photovoltaic conversion properties.[10,11] Currently, knowledge of the controlled chemical synthesis of monodisperse CZTS nanocrystals of defined phase and morphology is still very limited, which is disadvantageous for the further improvement of CZTS-based photovoltaic devices.

Up until now, monodisperse CZTS nanocrystals have been mainly synthesized by reacting metal salts with various sulfur sources[4−6,12−18] or by thermal decomposition of single-source precursors such as metal thiolate[19−23] and metal dithiocarbamate complexes[24−27] in suitable high-boiling-point solvents. Alkanethiols and fatty amines are the most commonly used solvents, in which the formation of unwanted binary and ternary products is suppressed while quaternary nanocrystals of high purity are obtained. Because of the complexity of the quaternary compound, reaction conditions should be accurately adjusted to control the composition and structure of CZTS nanocrystals. The reactions of metal salts with elemental sulfur[4−6,12−15] as well as thermal decomposition of metal dithiocarbamate complexes in oleylamine[24−27] at high temperatures usually lead to the formation of thermodynamically stable tetragonal kesterite CZTS nanocrystals. On the other hand, nanocrystals with a metastable hexagonal wurtzite structure are often prepared by reacting metal salts with alkanethiols[19−23] or thermal decomposition of metal dithiocarbamate complexes in the presence of alkanethiols.[26] The formation of hexagonal CZTS nanocrystals is often attributed to the induced growth from the preferentially formed Cu_xS nanocrystals due to the high reactivity of the Cu salt toward the sulfur precursor.[18,21,22,26] In short, precursors and surfactants used in the syntheses strongly influence the composition and crystallographic phase of the final CZTS nanocrystals. Phase-

Received: June 14, 2013
Published: November 22, 2013

ACS Publications © 2013 American Chemical Society

dx.doi.org/10.1021/ja405962k | J. Am. Chem. Soc. 2013, 135, 18377−18384

controlled synthesis of colloidal CZTS nanocrystals still remains a challenge, and more work is required to understand their growth mechanism.

In comparison to other sulfur sources, elemental sulfur is often preferred due to its low cost and ease of handling. Previously, sulfur dissolved in oleylamine (OM-S) has been used for the synthesis of CZTS nanocrystals, but with limited structural control, as only kesterite nanocrystals were obtained.[4−6,12−15] Herein, we report the phase-controlled synthesis of CZTS nanocrystals using elemental sulfur dissolved in octadecene (ODE-S) as the sulfur precursor in either dodecanethiol or oleylamine. The effects of sulfur activation by octadecene on the structure of the CZTS nanocrystals were studied in detail. Our results showed that CZTS nanocrystals can be changed from a kesterite to a wurtzite phase by increasing the reactivity of the sulfur precursors. Systematic investigations revealed that the reaction rate between the zinc precursor and sulfur precursor played a determining role in the formation of CZTS nanocrystals with different crystallographic phases.

EXPERIMENTAL SECTION

Materials. Analytical grade copper(II) acetate ($Cu(Ac)_2$), zinc acetate ($Zn(Ac)_2$), cadmium acetate ($Cd(Ac)_2$), manganese acetate ($Mn(Ac)_2$), zinc chloride ($ZnCl_2$), tin chloride ($SnCl_4$), sublimed sulfur (S), oleylamine (OM, 80%-90%), dodecene (DDE, 95%), and squalene (SE, 98%) were purchased from Aladdin Chemistry Co., Ltd. Copper(I) chloride (CuCl, ≥97%) was purchased from Shanghai Chemical Reagent Co., Ltd. Tin acetate ($Sn(Ac)_4$) was purchased from Alfa Aesar. 1-Dodecanethiol (DDT, ≥98%), octadecene (ODE, technical grade, 90%), and oleic acid (OA, technical grade, 90%) were purchased from Aldrich. 1,3-Diisopropenylbenzene (DIB, >97%) was purchased from TCI. H_2S (2%)/N_2 mixed gas was purchased from Shanghai WeiChuang Special Gas Co., Ltd. All chemicals were used as received without any further purification.

Preparation of ODE-S Precursor. Typically, a mixture of sulfur powder (4 mmol) and ODE (10 mL) was loaded into a 100 mL three-neck flask and heated to 155 °C under a nitrogen atmosphere to obtain a clear solution. The heating was maintained for 1 or 2 h to obtain a yellow or orange ODE-S solution, respectively. After that time, the mixture was cooled to room temperature naturally.

One-Step Synthesis of CZTS Nanocrystals in Dodecanethiol. For a typical one-step synthesis, $Cu(Ac)_2$ (1 mmol), $Zn(Ac)_2$ (0.5 mmol), $Sn(Ac)_4$ (0.5 mmol), OA (1 mL), and DDT (5 mL) were placed in a 100 mL three-neck flask. The reaction mixture was heated to 180 °C to form the metal−ligand complex under a nitrogen atmosphere. At this point, 5 mL of preformed ODE-S containing 2 mmol of S was rapidly injected into the mixture, resulting in immediate nanocrystal formation. The temperature of the mixture was then set to 240 °C for further growth. The reaction was allowed to proceed at 240 °C for 1 h. The obtained nanocrystals were isolated from the growth solution by precipitation with ethanol followed by centrifugation and redispersed in hexane. After several hexane/ethanol extractions, the final product was dispersed in hexane for further characterizations.

For the synthesis of CZTS nanocrystals using S powder as the sulfur source, a mixture of S powder and ODE was injected into the reaction mixture at 180 °C while other conditions were kept the same.

For the synthesis of CZTS nanocrystals using H_2S as the sulfur source, ODE was added at the beginning of the synthesis. H_2S/N_2 mixed gas was introduced into the reaction mixture at 180 °C with other procedures being the same.

For the synthesis of CZTS nanocrystals using metal chlorides as metal precursors, $Cu(Ac)_2$, $Zn(Ac)_2$, and $Sn(Ac)_4$ were replaced by equal amounts of CuCl, $ZnCl_2$,and $SnCl_4$. The reaction conditions were the same except that the injection temperature was reduced to 160 °C to avoid the formation of Cu_xS nanoparticles.

Two-Step Synthesis of CZTS Nanocrystals in Dodecanethiol. $Cu(Ac)_2$ (1 mmol), OA (1 mL), and DDT (5 mL) were placed in a 100 mL three-neck flask. The reaction mixture was heated to 180 °C to give a clear solution under a nitrogen atmosphere. Subsequently, 5 mL of an ODE-S solution containing 2 mmol of S was rapidly injected into the mixture. After injection, this first step of the reaction was allowed to proceed at 160 °C for 15 min. $Zn(Ac)_2$ (0.5 mmol) and $Sn(Ac)_4$ (0.5 mmol) were then simultaneously added to the solution. Finally, the reaction mixture was heated to 240 °C for 1 h for the second-step growth. Purification of the synthesized nanocrystals was similar to that described above in the one-step synthesis.

For the synthesis in which S first reacted with Cu and Sn precursors, $Sn(Ac)_4$ was added with $Cu(Ac)_2$ at the beginning of the synthesis, while the remaining $Zn(Ac)_2$ was added after the first-step reaction. All other procedures were the same as those described above.

For the synthesis in which S first reacted with Cu and Zn precursors, $Zn(Ac)_2$ was added with $Cu(Ac)_2$ at the beginning of the synthesis while the remaining $Sn(Ac)_4$ was added after the first-step reaction. All other procedures were kept the same.

Synthesis of CZTS Nanocrystals in Oleylamine. $Cu(Ac)_2$ (1 mmol), $Zn(Ac)_2$ (0.5 mmol), $Sn(Ac)_4$ (0.5 mmol), and OM (5 mL) were placed in a 100 mL three-neck flask. The reaction mixture was heated to 180 °C to form metal−ligand complexes under a nitrogen atmosphere. At this point, 5 mL of ODE-S containing 2 mmol of S was rapidly injected into the mixture. After the injection, the temperature of the mixture was raised to 240 °C and the reaction was continued for 1 h for further growth.

For the synthesis of CZTS nanocrystals using metal chlorides as metal precursors, $Cu(Ac)_2$, $Zn(Ac)_2$, and $Sn(Ac)_4$ were replaced by CuCl, $ZnCl_2$, and $SnCl_4$ of equal amounts, while all other experimental procedures were kept the same.

Characterizations. Transmission electron microscopy (TEM) and high-resolution transmission electron microscopy (HRTEM) images were taken with a FEI Technai G2 S-Twin instrument at an accelerating voltage of 200 kV. A sample for TEM analysis was prepared by placing a drop of the nanocrystal hexane solution on a carbon-coated copper grid and letting it dry in air. X-ray diffraction (XRD) analysis of drop-cast films of nanocrystals was conducted using a Bruker D8 Advance X-ray diffractometer (with Cu Kα radiation at 0.15418 nm). Energy-dispersive X-ray (EDX) analyses were performed using an EDAX X-ray detector attached to a Quanta 400 FEG scanning electron microscope. UV−vis absorption spectra were recorded on a Lambda-25 spectrometer. The spectra of ODE-S were recorded using ODE as reference. X-ray photoelectron spectroscopy (XPS) was carried out on a PHI 5000 VersaProbe spectrometer. The Raman spectra were recorded using a LABRAM HR confocal laser micro-Raman spectrometer.

Analysis of orange ODE-S was performed by using a ThermoFisher triple-quadrupole (TSQ) Vantage mass spectrometer and electrospray ionization (ESI) in the positive-ion mode. All samples were appropriately diluted in methanol with 20 μg/mL of $AgBF_4$ prior to direct infusion into the ESI chamber using a syringe pump at a flow rate of 5 μL/min.

RESULTS AND DISCUSSION

Preparation of ODE-S Precursor. ODE-S, prepared by dissolving elemental sulfur in ODE, is a well-known sulfur source for the synthesis of metal sulfide nanocrystals since Yu's work.[28] Both S and ODE are relatively environmentally friendly and economical. Nevertheless, the solubility of S powder in ODE is small at room temperature. To prepare a stable ODE-S precursor for the synthesis of CZTS nanocrystals, we heated a mixture of 4 mmol of S and 10 mL of ODE at 155 °C to accelerate sulfur dissolution. Interestingly, by prolonging the heating time, the mixture changed from colorless to yellow after about 1 h and then to orange after 2 h. These colored solutions were very stable after cooling, as shown in Figure 1. Only a small quantity of sulfur precipitated from the yellow ODE-S

dx.doi.org/10.1021/ja405962k | J. Am. Chem. Soc. 2013, 135, 18377−18384

Figure 1. Color photograph of yellow (left) and orange (right) ODE-S precursor solutions.

after storage overnight, while no S precipitation was observed in the orange ODE-S even after storage for several months. The observed color changes depended on the temperature and the absolute amount of S used. To obtain a similar orange ODE-S solution, ~4 h heating was required if the reaction temperature was lowered to 140 °C, while only 1 h was enough when a mixture of 2 mmol of S and 5 mL of ODE was heated at 155 °C. These colored ODE-S solutions were used as sulfur sources in the subsequent synthesis of CZTS nanocrystals.

Reactivity of Sulfur Precursor on the Phase Control of CZTS Nanocrystals. For the one-step synthesis of CZTS nanocrystals, the preformed colored ODE-S was injected into a solution of copper, zinc, and tin acetate in oleic acid and dodecanethiol at 180 °C, and then the reaction was carried out at 240 °C. It is interesting that the morphologies of the nanocrystals synthesized using different ODE-S precursors were different, as shown in Figure 2. When yellow ODE-S was

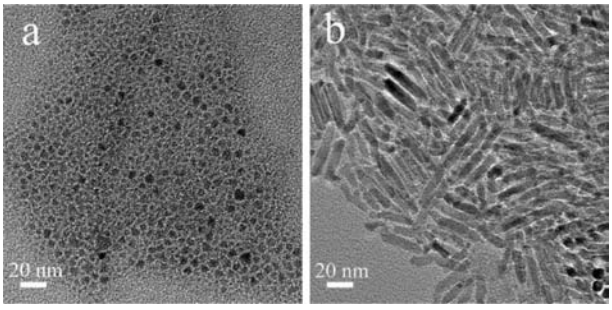

Figure 2. TEM images of the nanocrystals synthesized with yellow (a) and orange (b) ODE-S precursors.

used, small quasi-spherical and trigonal nanocrystals were formed (Figure 2a), while nanorods became the main products when orange ODE-S was used instead (Figure 2b).

Apart from the morphological differences, the composition and crystallographic structure of the two kinds of nanocrystals were also investigated. EDX (Figure S1, Supporting Information) and XPS (Figures S2 and S3, Supporting Information) analyses indicated that both types of nanocrystals were composed of Cu, Zn, Sn, and S. In addition, the Cu/Zn/Sn/S stoichiometric ratios were close to 2/1/1/4, and the oxidation states of all four elements were consistent with those of CZTS. Moreover, XRD analysis (Figure 3a) revealed that the nanocrystals synthesized with yellow ODE-S had a tetragonal kesterite structure, while those synthesized with orange ODE-S

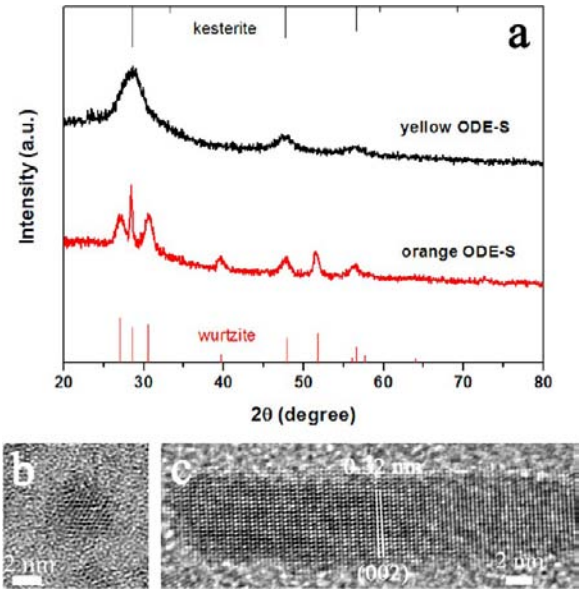

Figure 3. XRD patterns (a) and HRTEM images of the CZTS nanocrystals synthesized with yellow (b) and orange (c) ODE-S. The nanorods have a metastable wurtzite structure, growing along the [001] direction.

had a hexagonal wurtzite structure, which was further confirmed by an HRTEM analysis (Figure 3b,c). Given that binary and ternary compounds such as $Cu_{2-x}S$, ZnS, and Cu_2SnS_3 have similar XRD patterns overlapping with that of CZTS, Raman spectra were used to confirm the structure of the obtained product. As shown in Figure S4 (Supporting Information), both kinds of nanocrystals show a single Raman peak at ~330 cm^{-1}, which is close to the value reported for bulk CZTS, without any other characteristic impurity peaks, indicating they were not a mixture of Cu_2SnS_3 and ZnS.[29] Thus, both kinds of nanocrystals were CZTS nanocrystals, and the morphological difference between them was ascribed to their structural difference. Wurtzite nanocrystals with a hexagonal structure prefer to grow along the *c* axis, resulting in the formation of nanorods.[20] Furthermore, it was observed that the reactions between metal acetates and orange ODE-S precursor in the dodecanethiol system always led to the formation of wurtzite CZTS nanorods, as shown in Figure S5 (Supporting Information). Despite changes in the experimental conditions such as growth temperature and S injection temperature, only the size and yield of the nanorods varied. A typical UV−vis absorption spectrum of these CZTS nanorods is shown in Figure S6 (Supporting Information), and their direct band gap was determined to be 1.54 eV, while smaller CZTS nanocrystals synthesized with yellow ODE-S showed a larger band gap value due to the quantum confinement effect (data not shown).

Apparently, the key to our phase-controlled synthesis of CZTS nanocrystals is the utilization of ODE-S. Several groups have suggested that the crystal structure of the final CZTS nanocrystals was mainly determined by the structure of the initially formed Cu_xS nanocrystals,[18,26] as Cu is most reactive among the metal precursors. Nevertheless, we found the reaction between $Cu(Ac)_2$ with either yellow or orange ODE-S in dodecanethiol resulted in the formation of the same $Cu_{1.8}S$ nanocrystals (Figure S7, Supporting Information). Moreover, further growth after subsequent simultaneous addition of

dx.doi.org/10.1021/ja405962k | J. Am. Chem. Soc. 2013, 135, 18377−18384

$Sn(Ac)_4$ and $Zn(Ac)_2$ led to the formation of wurtzite nanocrystals (Figure S8, Supporting Information), regardless of the type of ODE-S used. Therefore, the different structures of CZTS nanocrystals were not related to different Cu_xS nanocrystal seeds in our experimental system.

To further investigate the role the S source played in the syntheses, other S sources were used to prepare CZTS nanocrystals. It was found that small kesterite nanocrystals were obtained when a mixture of ODE and S powder was used (Figure S9, Supporting Information), indicating that the preparation of colored ODE-S was not simple dissolution of S powder in ODE but a chemical reaction between S and ODE. The activation of elemental S by ODE in the synthesis of sulfide nanocrystals has been previously reported,[30,31] and Li et al. suggested that H_2S generated from the reduction of S by ODE at 180 °C was the real S precursor in the formation of CdS nanocrystals.[31] Although the reaction between metal acetates and H_2S in DDT did result in the formation of wurtzite CZTS nanocrystals (Figure S10, Supporting Information), the much lower activation temperature of S used in our work (140−160 °C) was not sufficient to generate a large amount of H_2S.

The color change in the preparation of ODE-S was reminiscent of the formation of polysulfide ions (S_n^{2-}) in the well-known reaction between S and NaOH aqueous solution. With increasing n, the S_n^{2-} solution turns from yellow to orange and then to red. Moreover, a survey of literature from the 1940s revealed that the reactions of S and olefins generally lead to the formation of organic polysulfides (RS_nR).[32,33] Comparing the UV−vis absorption spectra of the ODE-S precursors (Figure 4)

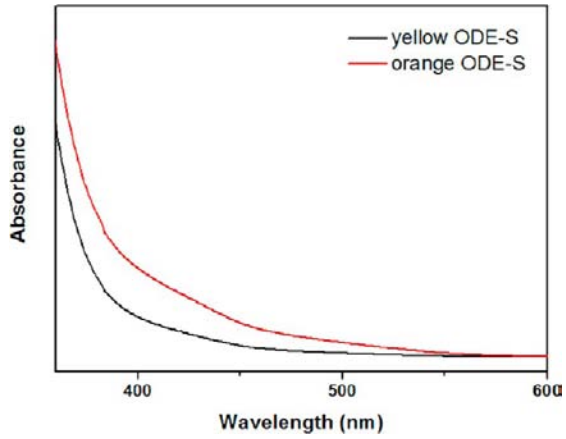

Figure 4. UV−vis absorption spectra of the ODE-S precursor solutions. The spectrum of orange ODE-S shifts to longer wavelength due to the existence of polysulfides with long S chains.

with the calculated spectra[34] of polysulfide, we propose that orange ODE-S contained RS_xR ($x \geq 3$). Preliminary results from the ESI-MS characterization of orange ODE-S showed the possible existence of $(C_{18}H_{35})_2S_5$ and $(C_{18}H_{35})_2S_{10}$ (Figure S11, Supporting Information), although more detailed investigations are still needed to accurately identify the active species in the prepared ODE-S precursors, by developing a better method to ionize these organic polysulfide species for more efficient detection. We believe the existence of polysulfides with long S chains makes the orange ODE-S more reactive than its yellow counterpart, as the S−S bond in long sulfur chains is much weaker than that in S_8 rings,[35] which was confirmed by the experimental result that the reaction between orange ODE-S and $Cu(Ac)_2$ led to the formation of smaller $Cu_{1.8}S$ nanocrystals (Figure S7, Supporting Information). It is worth noting that wurtzite CZTS nanocrystals could also be synthesized using polysulfides prepared by the reactions between sulfur and other olefins such as DDE, SE, and DIB (Figure S12, Supporting Information). More specifically, poly(sulfur-random-(1,3-diisopropenylbenzene)) (poly(S-r-DIB)) with extensive polymeric sulfur structures[36] produced small wurtzite CZTS, likely due to the high reactivity of the polymeric sulfur inducing fast nucleation. Therefore, the phase-controlled synthesis of CZTS nanocrystals was related to the specific reactivity of sulfur precursors. When low-reactivity yellow ODE-S was used, kesterite CZTS nanocrystals were formed. In contrast, the use of more reactive orange ODE-S led to the formation of wurtzite CZTS nanocrystals.

In order to isolate and analyze the nanocrystals at the nucleation stage, we quenched the reaction by adding cold hexane immediately after the injection of ODE-S in a one-step synthesis of CZTS nanocrystals. The purified nuclei were analyzed by EDX to investigate their compositions. It was revealed that the average compositions of the CZTS nuclei for the injection of yellow and orange ODE-S were $Cu_2Zn_{0.84}Sn_{1.14}S_{6.17}$ and $Cu_2Zn_{0.96}Sn_{0.67}S_{5.96}$, respectively. This showed that the nuclei of wurtzite CZTS nanocrystals were relatively Cu and Zn rich, indicating that the Cu and Zn precursors reacted with S precursors faster in comparison to Sn due to the use of the more reactive orange ODE-S. The large excess of sulfur content was likely due to the large number of thiol molecules capping on the surface of these small nuclei, which would decrease to near stoichiometric values as nanoparticles grew in size.

According to the hard−soft acid−base theory,[37] Cu^+, Zn^{2+}, and Sn^{4+} are soft, intermediate, and hard Lewis acids, respectively. Therefore, their reactivity toward the soft Lewis base S precursor should be in the order $Cu^+ > Zn^{2+} > Sn^{4+}$. However, this reactivity order is often not followed in the synthesis of CZTS nanocrystals. There are two possible reasons. First, the coordination of the capping ligands in the reaction system can alter the reactivity of the metal precursors. For example, the presence of DDT can reduce the reactivity of the Cu precursor.[38] Second, the preferential formation of a ternary Cu−Sn−S compound may lower the thermodynamic energy of the reaction, causing the reaction between Sn and S to proceed more quickly than that between Zn and S, which is often observed in the synthesis of CZTS nanocrystals.[14] In our system, when yellow ODE-S was used, the nuclei were Sn rich owing to the above reasons. In contrast, when the more reactive orange ODE-S was used, the reaction between the S precursor and the softer Cu and Zn precursors was accelerated significantly, resulting in the formation of Cu- and Zn-rich nuclei. On the basis of the results above, we conclude that phase-controlled synthesis of CZTS nanocrystals can be realized by tuning the relative reaction rates between different metal precursors and the S precursor.

Reactivity of Metal Precursor on the Phase Control of CZTS Nanocrystals. The reaction rate between the metal precursor and S precursor is influenced not only by the reactivity of the S precursor but also by that of the metal precursor, which can be tuned by adding different ligands.[39,40] To investigate the effect of relative reactivity between metal and S precursors on the structure of the CZTS nanocrystals, metal chlorides were used instead of acetates in the synthesis. Cl^- is a

hard base; therefore, CuCl will be more reactive than $Cu(Ac)_2$, which is confirmed by the lower reaction temperature needed for CuCl with DDT in comparison with that for $Cu(Ac)_2$ (~175 °C versus ~200 °C). Meanwhile, $ZnCl_2$ should be less reactive than $Zn(Ac)_2$ due to the strong complexation between chloride ions and zinc ions. As a result, the relative reaction rate between the Cu precursor and ODE-S should be increased, while the reaction between the Zn precursor and ODE-S should be slower when chlorides are used. The results in Figure 5 show that the reactions between metal chlorides and both

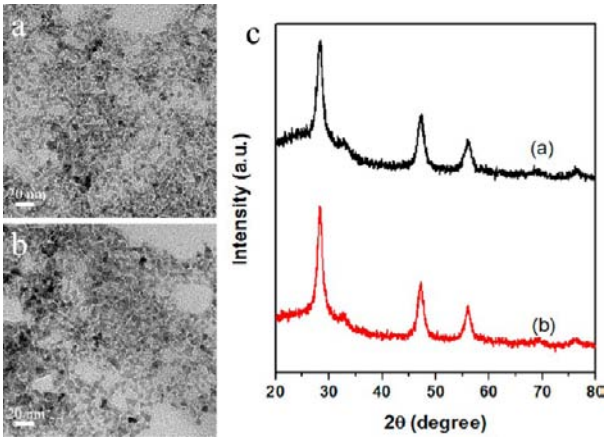

Figure 5. TEM images (a, b) and XRD patterns (c) of the CZTS nanocrystals synthesized using metal chlorides in dodecanethiol with yellow (a) and orange (b) ODE-S.

types of ODE-S indeed all led to the formation of kesterite nanocrystals, suggesting that a fast reaction between zinc and sulfur precursors is necessary for the formation of wurtzite CZTS nanocrystals in our reaction system.

Two-Step Synthesis of CZTS Nanocrystals in Dodecanethiol. To further prove the hypothesis that relatively Zn rich CZTS nuclei favor the formation of nanocrystals with a wurtzite structure, additional two-step syntheses were carried out. In these experiments, ODE-S first reacted with $Cu(Ac)_2$ and another metal acetate ($M(Ac)_x$) to form Cu−M−S nanocrystal intermediates, and then the third metal acetate was added for further second-step growth. The TEM images and XRD patterns of the obtained CZTS nanocrystals are shown in Figure 6. When ODE-S was first reacted with $Cu(Ac)_2$ and $Sn(Ac)_4$, the use of yellow ODE-S led to the formation of small kesterite nanocrystals, while pure wurtzite nanorods were obtained for orange ODE-S, similar to the results shown in Figure 2, indicating that the reaction between the Zn precursor and ODE-S is indeed determining for the phase-controlled synthesis of CZTS nanocrystals. When yellow ODE-S was used, Zn entered into the nanocrystal structure very slowly owing to the slow reaction rate between the Zn and S precursors, favoring the formation of kesterite CZTS nanocrystals. In contrast, the use of orange ODE-S accelerated Zn entry into the nanocrystals, leading to the formation of wurtzite CZTS nuclei. The results for ODE-S first reacting with $Cu(Ac)_2$ and $Zn(Ac)_2$ further supported this hypothesis. As expected, wurtzite CZTS nanocrystals were obtained for both types of ODE-S due to the formation of relatively Zn rich nuclei in this case.

Owing to the relatively lower reactivity of Zn and Sn toward S in dodecanethiol, no secondary homogeneous self-nucleation

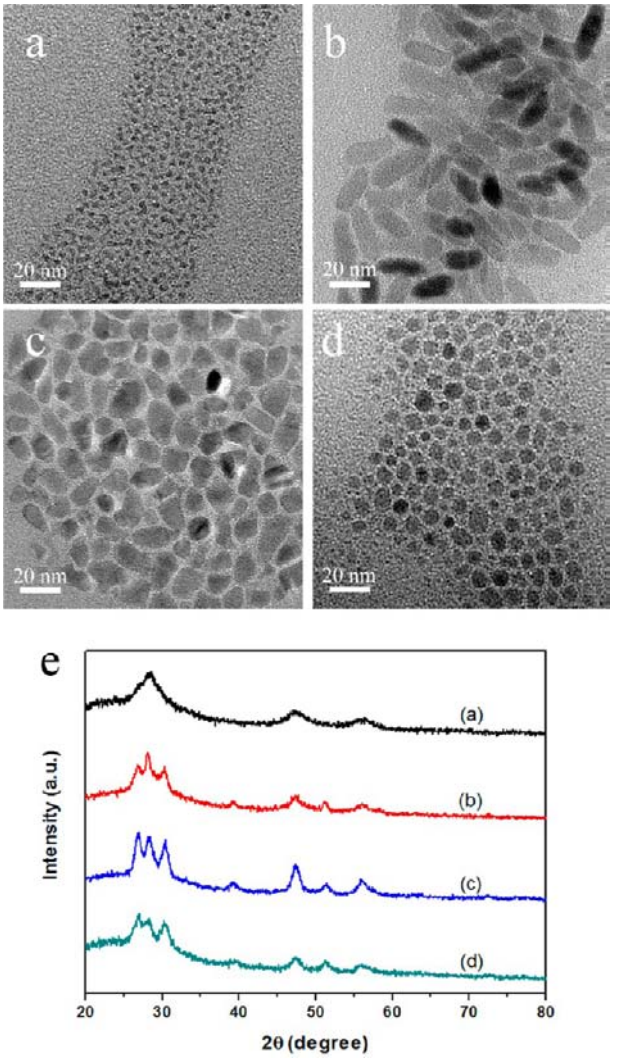

Figure 6. TEM images (a−d) and XRD patterns (e) of the CZTS nanocrystals synthesized by two-step reaction in dodecanethiol with $Cu(Ac)_2$ and $Sn(Ac)_4$ first added and yellow (a) or orange (b) as the S source, and with $Cu(Ac)_2$ and $Zn(Ac)_2$ first added and yellow (c) or orange (d) ODE-S as the S source.

was observed at the second-step growth stage. Moreover, in the case of Cu−Zn−S nuclei induced growth, wurtzite CZTS nanocrystals were obtained for both ODE-S species, but the use of the more reactive orange ODE-S led to the formation of more Cu−Zn−S nuclei with smaller sizes, which in turn resulted in smaller CZTS nanocrystals synthesized with orange ODE-S (Figure 6d) in comparison to those with yellow ODE-S (Figure 6c).

Phase-Controlled Synthesis of CZTS Nanocrystals in Oleylamine. In addition to alkanethiols, fatty amines are also often chosen as the solvents in the synthesis of copper-based chalcogenide nanocrystals. Regulacio et al. have found that thermal decomposition of metal dithiocarbamate complexes in hexadecanethiol led to the formation of wurtzite-related CZTS nanocrystals, while zinc blende derived CZTS nanocrystals were obtained in oleylamine.[26] To investigate the effect of solvents on the structure of CZTS nanocrystals in our system, oleylamine was substituted for dodecanethiol in the synthesis.

XRD patterns of CZTS nanocrystals synthesized using different precursors in oleylamine are shown in Figure 7e,

dx.doi.org/10.1021/ja405962k | J. Am. Chem. Soc. 2013, 135, 18377−18384

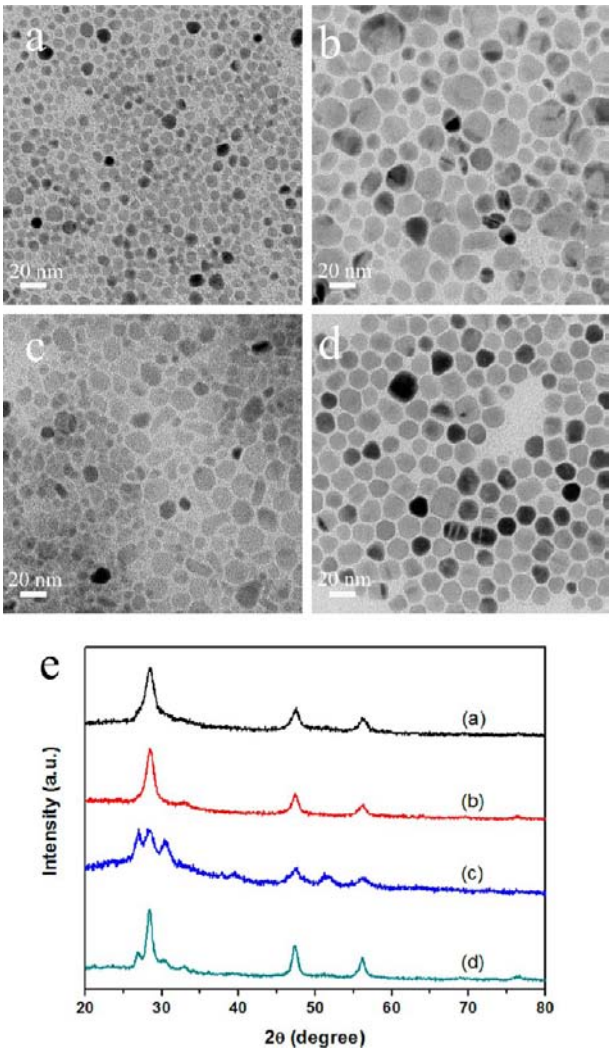

Figure 7. TEM images (a–d) and XRD patterns (e) of the CZTS nanocrystals synthesized in oleylamine with metal acetates and yellow ODE-S (a), metal chlorides and yellow ODE-S (b), metal acetates and orange ODE-S (c), and metal chlorides and orange ODE-S (d) as precursors.

which are similar to the results of using dodecanethiol as solvent. The use of yellow ODE-S always led to the formation of kesterite CZTS nanocrystals. When orange ODE-S acted as the sulfur source, the anions of the metal salts determined the structure of CZTS nanocrystals. The reaction between orange ODE-S and metal acetates resulted in the formation of wurtzite CZTS nanocrystals, while kesterite nanocrystals were the main products of the reaction between orange ODE-S and metal chlorides, although some wurtzite nanocrystals also existed. The TEM images shown in Figure 7a–d revealed that the kesterite CZTS nanocrystals obtained in oleylamine were larger than those synthesized in dodecanethiol and most of the wurtzite nanocrystals were nanoplates rather than nanorods, indicating that dodecanethiol played an important role in the formation of nanorods. The increase of the size of the nanocrystals indicated that oleylamine influenced the reactivity of the precursors to some extent, but the change in the relative reaction rate between each metal and the S precursor was small. Thus, in our system, the solvent effect on the structure of CZTS nanocrystals was not as strong as the effect of the reaction rate between zinc and sulfur precursors.

Reaction between Zn and S Precursors Being the Key to Phase-Controlled Synthesis of CZTS Nanocrystals. Up to now, significant research advancement has been achieved in the synthesis of CZTS nanocrystals, but the phase determination is still perplexing. For example, the use of oleylamine as solvent is necessary for the formation of wurtzite CZTS nanocrystals by thermal decomposition of metal thiolates,[21,23] but the same oleylamine leads to the formation of kesterite CZTS nanocrystals in the thermal decomposition of metal dithiocarbamate complexes.[24−27] In general, the combination of reaction variables rather than any single one in the reaction system determines the structure of the final nanocrystals. To realize the phase-controlled synthesis of CZTS nanocrystals, the reaction rates between different metal precursors and sulfur precursors should be accurately tuned by selecting proper precursors and ligands.

Shavel et al. found that the kinetics of the reaction of each element with a sulfur precursor is fastest for Cu and slowest for Zn in forming kesterite CZTS nanocrystals when reacting metal salts with elemental sulfur in oleylamine.[14] In the synthesis of wurtzite CZTS nanocrystals by thermal decomposition of metal thiolates in the presence of oleylamine, Li et al. found Zn was preferentially doped into initially formed Cu_2S nanocrystals over Sn.[21] These experimental results indicate the preferential reaction between Sn and S resulted in the formation of kesterite nanocrystals while wurtzite nanocrystals were obtained when the reaction between Zn and S was faster. Additionally, it was reported that the reaction between metal chlorides and thiourea in oleylamine resulted in the formation of pure kesterite CZTS nanocrystals,[16] while a mixture of kesterite and wurtzite CZTS nanocrystals were obtained when metal acetates were reacted with thiourea in oleylamine,[17] also confirming the importance of increasing the reactivity of the Zn precursor for the formation of wurtzite CZTS nanocrystals.

In previous reports, the faster kinetics of the reaction with the sulfur precursor for Zn was often attributed to the preferential formation of Cu_2S nanocrystals.[21,22,26] Li et al. suggested that because the ionic radius of Zn^{2+} was closer to that of Cu^+ than to that of Sn^{4+}, the entry of Zn^{2+} into the Cu_2S nanocrystal structure was faster when no strong ligand such as Cl^- existed in the reaction system.[21] In this work, we find the reaction between Zn and S precursors can also be accelerated by increasing the reactivity of the S precursor, on the basis of the results of one-step and two-step syntheses of CZTS nanocrystals with emphasis on the dodecanethiol system. CZTS nanocrystals with a wurtzite structure are formed due to a faster reaction between Zn and S precursors when orange ODE-S is used (Scheme 1). In contrast, the use of yellow ODE-S or the addition of strong ligands leads to the formation of kesterite nanocrystals. Very recently, Cattley et al. synthesized wurtzite CZTS nanoparticles by reacting amine complexes of metal salts with the highly reactive sulfur precursor bis-(trimethylsilyl) sulfide at relatively low temperatures,[18] which is consistent with our observations. Why the Zn-rich nuclei favor the formation of wurtzite CZTS nanocrystals is still not clear. Perhaps, Zn-rich CZTS nuclei with a wurtzite structure are more stable or kinetically favored than those in a kesterite structure. Another possibility is that the structure of preferentially formed Cu–Zn–S nanocrystals is close to that of hexagonal Cu_2S or hexagonal ZnS, as the exchange of Cu^+ and Zn^{2+} ions in the crystal lattice is energetically inexpensive, owing to their similar physical properties.[8,26]

dx.doi.org/10.1021/ja405962k | J. Am. Chem. Soc. 2013, 135, 18377−18384

Scheme 1. Schematic Diagram of the Proposed Mechanism of Phase-Controlled Synthesis of CZTS Nanocrystals[a]

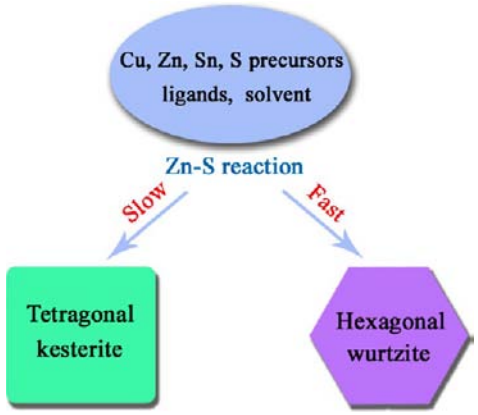

[a]The crystallographic phases are determined by the reaction order of each metal and sulfur precursor. A preference for the Zn−S reaction over the Sn−S reaction favors the formation of a metastable hexagonal wurtzite structure.

Quaternary Cu_2MSnS_4 (M = Cd^{2+}, Mn^{2+}) was also synthesized with orange ODE-S to investigate the effect of the reaction rate between M^{2+} ions and S precursors in the phase control of these nanocrystals (Figure S13, Supporting Information). Similar to the case for CZTS, the obtained Cu_2CdSnS_4 nanocrystals have a wurtzite structure. In contrast, most Cu_2MnSnS_4 nanocrystals possess a kesterite structure. It is known that Cd^{2+} is softer while Mn^{2+} is harder than Zn^{2+}. Therefore, kesterite Cu_2MnSnS_4 nanocrystals were formed due to the relatively slow Mn−S reaction despite the fact that the reactive orange ODE-S was used, confirming the fast reaction between M^{2+} ions and S precursors is determining in the formation of not only wurtzite Cu_2ZnSnS_4 nanocrystals but also other wurtzite Cu_2MSnS_4 nanocrystals.

Differences in passivation of certain crystallographic facets can lead to different nanocrystal shapes and sometimes crystal structures, as reported in the literature.[41] However, the possibility that interactions between ODE-S and the crystal facets of nanocrystals determine the final structure of CZTS nanocrystals in the current experimental system is small, as we have also prepared wurtzite nanocrystals with yellow ODE-S (Figure 6c and Figure S8a (Supporting Information)), as well as kesterite nanocrystals with orange ODE-S by first preparing tetragonal Cu_2SnS_3, and then further reacting with Zn (data not shown).

Finally, although we have proven that the fast reaction between Zn and S precursors is determining for the growth of wurtzite CZTS nanocrystals in our system, it is still difficult to say that this is the only condition for the formation of wurtzite CZTS nanocrystals. Recently, the synthesis of hexagonal Cu−Sn−S nanocrystals has been reported,[42,43] which may also induce the preferential growth of hexagonal CZTS nanocrystals. Therefore, more work is still needed to fully understand the growth mechanism of CZTS nanocrystals, especially on the effect of the structure of preferentially formed Cu_xS and/or Cu_2SnS_3 nanocrystals.

CONCLUSION

Phase-controlled synthesis of CZTS nanocrystals has been realized by the reaction between metal salts and ODE-S in either dodecanethiol or oleylamine. We find that elemental sulfur can react with ODE, producing sulfur precursors (yellow or orange ODE-S) with different reactivities toward metal ions, which is likely due to the formed organic polysulfides. The use of yellow ODE-S leads to the formation of kesterite CZTS nanocrystals, while wurtzite CZTS nanocrystals are obtained by using the more reactive orange ODE-S. A systematic investigation has shown that the formation of metastable wurtzite CZTS nanocrystals is favored by relatively Zn rich nuclei, which resulted from the fast reaction between Zn and S precursors in our experimental system. We propose that the relatively faster Zn−S reaction (in comparison to the Sn−S reaction), in other words, avoiding the preferential nucleation of Cu- and Sn-rich tetragonal nanocrystals, is necessary for wurtzite CZTS nanocrystal formation. Moreover, this mechanism for phase control can be extended to other quaternary Cu_2MSnS_4 (M = Cd^{2+}, Mn^{2+}) nanocrystal syntheses, where the relative reactivities of M^{2+} and sulfur precursors play a key role.

ASSOCIATED CONTENT

Supporting Information

Figures giving EDX, XPS, Raman, and UV−vis absorption spectra of CZTS nanocrystals, additional XRD patterns and TEM images of CZTS nanocrystals synthesized under other experimental conditions, ESI-MS of orange ODE-S, and the characterization of $Cu_{1.8}S$, Cu_2CdSnS_4, and Cu_2MnSnS_4 nanocrystals. This material is available free of charge via the Internet at http://pubs.acs.org.

AUTHOR INFORMATION

Corresponding Author

jjiang2010@sinano.ac.cn

Author Contributions

The manuscript was written through contributions of all authors./All authors have given approval to the final version of the manuscript. /

Notes

The authors declare no competing financial interest.

ACKNOWLEDGMENTS

This work was funded by the "Hundred Talents" program of the Chinese Academy of Sciences and the Natural Science Foundation of China (Grant No. 51202283). We thank the Medical College of Soochow University for providing the mass spectrometry facility support.

REFERENCES

(1) Hillhouse, H. W.; Beard, M. C. *Curr. Opin. Colloid Interface Sci.* **2009**, *14*, 245.
(2) Sargent, E. H. *Nat. Photonics* **2012**, *6*, 133.
(3) Peng, X. *Nano Res.* **2009**, *2*, 425.
(4) Riha, S. C.; Parkinson, B. A.; Prieto, A. L. *J. Am. Chem. Soc.* **2009**, *131*, 12054.
(5) Guo, Q.; Hillhouse, H. W.; Agrawal, R. *J. Am. Chem. Soc.* **2009**, *131*, 11672.
(6) Steinhagen, C.; Panthani, M. G.; Akhavan, V.; Goodfellow, B.; Koo, B.; Korgel, B. A. *J. Am. Chem. Soc.* **2009**, *131*, 12554.
(7) Katagiri, H.; Jimbo, K.; Maw, W. S.; Oishi, K.; Yamazaki, M.; Araki, H.; Takeuchi, A. *Thin Solid Films* **2009**, *517*, 2455.
(8) Siebentritt, S.; Schorr, S. *Prog. Photovoltaics* **2012**, *20*, 512.
(9) Guo, Q.; Ford, G. M.; Yang, W.-C.; Walker, B. C.; Stach, E. A.; Hillhouse, H. W.; Agrawal, R. *J. Am. Chem. Soc.* **2010**, *132*, 17384.
(10) Huynh, W. U.; Dittmer, J. J.; Alivisatos, A. P. *Science* **2002**, *295*, 2425.

(11) Salant, A.; Shalom, M.; Tachan, Z.; Buhbut, S.; Zaban, A.; Banin, U. *Nano Lett.* **2012**, *12*, 2095.
(12) Kameyama, T.; Osaki, T.; Okazaki, K.-i.; Shibayama, T.; Kudo, A.; Kuwabata, S.; Torimoto, T. *J. Mater. Chem.* **2010**, *20*, 5319.
(13) Rath, T.; Haas, W.; Pein, A.; Saf, R.; Maier, E.; Kunert, B.; Hofer, F.; Resel, R.; Trimmel, G. *Sol. Energy Mater. Sol. Cells* **2012**, *101*, 87.
(14) Shavel, A.; Cadavid, D.; Ibáñez, M.; Carrete, A.; Cabot, A. *J. Am. Chem. Soc.* **2012**, *134*, 1438.
(15) Yang, H.; Jauregui, L. A.; Zhang, G.; Chen, Y. P.; Wu, Y. *Nano Lett.* **2012**, *12*, 540.
(16) Wei, M.; Du, Q.; Wang, D.; Liu, W.; Jiang, G.; Zhu, C. *Mater. Lett.* **2012**, *79*, 177.
(17) Sarswat, P. K.; Free, M. L. *J. Cryst. Growth* **2013**, *372*, 87.
(18) Cattley, C. A.; Cheng, C.; Fairclough, S. M.; Droessler, L. M.; Young, N. P.; Warner, J. H.; Smith, J. M.; Assender, H. E.; Watt, A. A. R. *Chem. Commun.* **2013**, *49*, 3745.
(19) Lu, X.; Zhuang, Z.; Peng, Q.; Li, Y. *Chem. Commun.* **2011**, *47*, 3141.
(20) Singh, A.; Geaney, H.; Laffir, F.; Ryan, K. M. *J. Am. Chem. Soc.* **2012**, *134*, 2910.
(21) Li, M.; Zhou, W.-H.; Guo, J.; Zhou, Y.-L.; Hou, Z.-L.; Jiao, J.; Zhou, Z.-J.; Du, Z.-L.; Wu, S.-X. *J. Phys. Chem. C* **2012**, *116*, 26507.
(22) Liao, H.-C.; Jao, M.-H.; Shyue, J.-J.; Chen, Y.-F.; Su, W.-F. *J. Mater. Chem. A* **2013**, *1*, 337.
(23) Chang, J.; Waclawik, E. R. *CrystEngComm* **2013**, *15*, 5612.
(24) Zou, C.; Zhang, L.; Lin, D.; Yang, Y.; Li, Q.; Xu, X.; Chen, X. a.; Huang, S. *CrystEngComm* **2011**, *13*, 3310.
(25) Khare, A.; Wills, A. W.; Ammerman, L. M.; Norris, D. J.; Aydil, E. S. *Chem. Commun.* **2011**, *47*, 11721.
(26) Regulacio, M. D.; Ye, C.; Lim, S. H.; Bosman, M.; Ye, E.; Chen, S.; Xu, Q.-H.; Han, M.-Y. *Chem. Eur. J.* **2012**, *18*, 3127.
(27) Chesman, A. S. R.; van Embden, J.; Duffy, N. W.; Webster, N. A. S.; Jasieniak, J. J. *Cryst. Growth Des.* **2013**, *13*, 1712.
(28) Yu, W. W.; Peng, X. *Angew. Chem., Int. Ed.* **2002**, *41*, 2368.
(29) Fernandes, P. A.; Salomé, P. M. P.; da Cunha, A. F. *J. Alloys Compd.* **2011**, *509*, 7600.
(30) Yordanov, G.; Yoshimura, H.; Dushkin, C. *Colloid Polym. Sci.* **2008**, *286*, 813.
(31) Li, Z.; Ji, Y.; Xie, R.; Grisham, S. Y.; Peng, X. *J. Am. Chem. Soc.* **2011**, *133*, 17248.
(32) Armstrong, R. T.; Little, J. R.; Doak, K. W. *Ind. Eng. Chem.* **1944**, *36*, 628.
(33) Farmer, E. H.; Shipley, F. W. *J. Chem. Soc.* **1947**, 1519.
(34) Bosser, G.; Anouti, M.; Paris, J. *J. Chem. Soc., Perkin Trans. 2* **1996**, 1993.
(35) Hodgson, W. G.; Buckler, S. A.; Peters, G. *J. Am. Chem. Soc.* **1963**, *85*, 543.
(36) Chung, W. J.; Griebel, J. J.; Kim, E. T.; Yoon, H.; Simmonds, A. G.; Ji, H. J.; Dirlam, P. T.; Glass, R. S.; Wie, J. J.; Nguyen, N. A.; Guralnick, B. W.; Park, J.; Somogyi, A.; Theato, P.; Mackay, M. E.; Sung, Y.-E.; Char, K.; Pyun, J. *Nat. Chem.* **2013**, *5*, 518.
(37) Pearson, R. G. *J. Am. Chem. Soc.* **1963**, *85*, 3533.
(38) Xie, R.; Rutherford, M.; Peng, X. *J. Am. Chem. Soc.* **2009**, *131*, 5691.
(39) Zhong, H.; Lo, S. S.; Mirkovic, T.; Li, Y.; Ding, Y.; Li, Y.; Scholes, G. D. *ACS Nano* **2010**, *4*, 5253.
(40) Kuzuya, T.; Hamanaka, Y.; Itoh, K.; Kino, T.; Sumiyama, K.; Fukunaka, Y.; Hirai, S. *J. Colloid Interface Sci.* **2012**, *388*, 137.
(41) Kumar, S.; Nann, T. *Small* **2006**, *2*, 316.
(42) Liu, Q.; Zhao, Z.; Lin, Y.; Guo, P.; Li, S.; Pan, D.; Ji, X. *Chem. Commun.* **2011**, *47*, 964.
(43) Yi, L.; Wang, D.; Gao, M. *CrystEngComm* **2012**, *14*, 401.